Electronic Supplementary Material (ESI) for Soft Matter.

Supporting Information

Cellulose Nanocrystals for Gelation and Percolation-induced Reinforcement of a Photocurable Poly (vinyl alcohol) Derivative

Ria D. Corder,[1*] Prajesh Adhikari,[1*] Michael C. Burroughs,[1†] Orlando J. Rojas,[1,2,3‡] and Saad A. Khan[1‡]

[1]Department of Chemical and Biomolecular Engineering, North Carolina State University, Raleigh, NC 27695, USA

[2]Department of Bioproducts and Biosystems, School of Chemical Engineering, Aalto University, Espoo, FI-00076, Finland

[3]Bioproducts Institute, Department of Chemical and Biological Engineering, Chemistry and Wood Science, University of British Columbia, Vancouver BC V6T 1Z3, Canada

[*] Co-first authors.

[†] Current address: Department of Chemical Engineering, University of California Santa Barbara, Santa Barbara, CA, 93106.

[‡] Corresponding authors (email: orlando.rojas@ubc.ca; khan@eos.ncsu.edu).

Images of Dilute CNC Dispersions With and Without PVA-SbQ

The effect of PVA-SbQ addition on the visual appearance of 0.1 and 0.5 wt% CNC dispersions is given in **Figure S1**. The presence of 0.45 wt% (100 μM) PVA-SbQ causes the dispersions to turn cloudy, indicating the presence of aggregates.

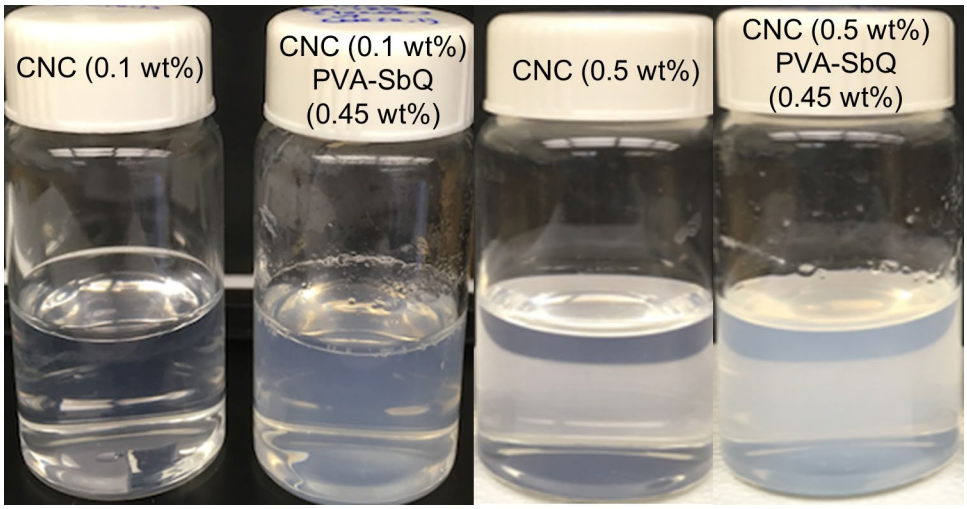

Figure S1. Images of CNC (0.1 wt%), CNC (0.1 wt%) with PVA-SbQ (0.45 wt%), CNC (0.5 wt%), and CNC (0.5 wt%) with PVA-SbQ (0.45 wt%) in 20 mL scintillation vials.

Calculation of the Theoretical Hydrodynamic Radius for CNCs using the Stokes-Einstein Equation and Kirkwood-Riseman Theory

The hydrodynamic radius (R_h) of a particle, defined as the size of a diffusion-equivalent sphere, can be calculated according to the Stokes-Einstein equation (Equation S1):

$$R_h = \frac{KT}{6\pi\eta D_t} \qquad \text{(S1)}$$

where K is Boltzmann's constant, T is the absolute temperature, η is viscosity, and D_t is the translational diffusion coefficient.[1]

The Kirkwood- Riseman theory[2] can be used to approximate D_t for rod-shaped macromolecules of length (L) and diameter (d) in dilute solution according to Equation S2:

$$D_t = \frac{KT}{3\pi \mathrm{L}} \ln\left(\frac{L}{d}\right) \qquad \text{(S2)}$$

Combining Equations 1 and 2 results in the following expression for R_h (Equation S3):

$$R_h = \frac{L}{2\ln\left(\frac{L}{d}\right)} \qquad \text{(S3)}$$

Using the manufacturer-reported dimensions for the CNC used this work (L = 100 nm, d = 5 nm), R_h is estimated to be 16.7 nm.

Steady-Shear Rheology of CNC Dispersions

The effect of CNC concentration in DI water on apparent viscosity (η) over several decades of shear rate (10^{-2}-10^{2} s^{-1}) is shown in **Figure S2**. The most prominent features for 1-3 wt% CNCs include a small Newtonian plateau for 1 wt% (which disappears at higher concentrations), a steep shear-thinning region at low shear rates (< 1 s^{-1}) and a further shear-thinning region at higher shear rates. The second shear-thinning regime is less steep, a trend commonly observed for lyotropic polymer liquid crystals.[3] For 6.7 wt% CNCs, the slopes of the shear-thinning regions at low and high shear rates become similar. This behavior has been the subject of numerous previous rheological studies and has been attributed to gel formation, which impedes the formation of chiral-nematic ordered phases.[4–6]

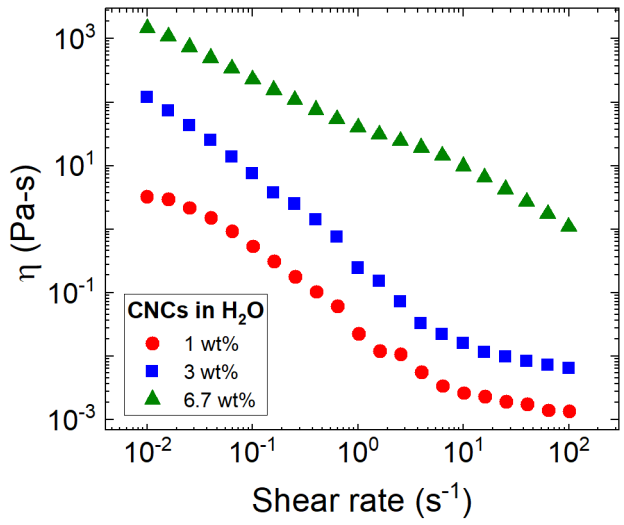

Figure S2. Steady-shear viscosity (η) results for CNCs dispersed in DI water at different concentrations (data sets labeled and color-coded).

Calculation of Intrinsic Viscosity using the Huggins Equation

The steady-shear rheological behavior of dispersions containing rod-like structures such as CNCs is predominantly influenced by stresses related to the suspending medium as well as the particle. In dilute dispersions, where colloidal interactions can be neglected, particle properties such as size, shape, size distribution, stiffness and deformability influence viscosity by affecting the tendency to align into ordered phases under shear flow. The intrinsic viscosity ([η]) of CNC was calculated using the Huggins equation,[7] given below as Equation S4:

$$\frac{\eta_{sp}}{c} = [\eta] + k_H[\eta]^2 \quad \text{(S4)}$$

where η_{sp} is the specific viscosity, c is the concentration of CNCs in water, and k_h is the Huggins coefficient. By plotting (η_{sp}/c) versus c as shown below in **Figure S3** for CNC concentrations in the dilute regime, [η] can be estimated from the y-intercept of a linear fit of the data. Using this method, [η] was estimated as 47.3 mL/g, yielding k_H = 1.39.

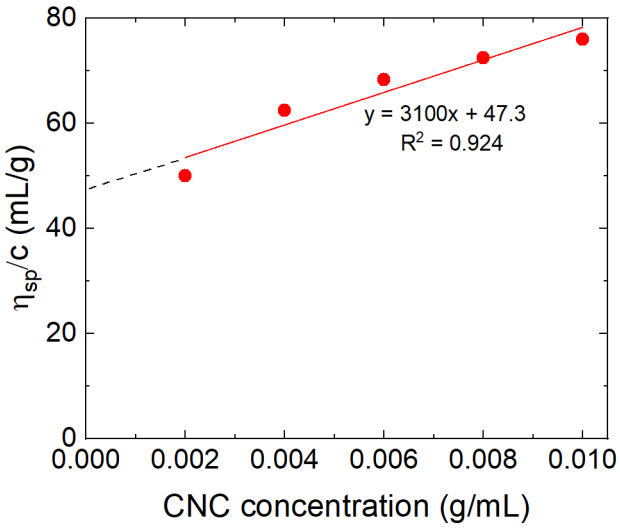

Figure S3. (a) Huggins plot of specific viscosity divided by concentration (η_{sp}/c) vs. CNC concentration, used to determine intrinsic viscosity ([η]). The solid red line represents a linear fit to the data, while the dashed black line denotes an extrapolation of the linear fit to the y-axis to obtain [η] = 47.3 mL/g.

CNC Aspect Ratio Calculation using Simha's Equation

The axial ratio of the ellipsoid (ratio of the long radius to the short radius) of suspended particles can be calculated using Simha's equation for prolate ellipsoids,[8] given below as Equation S5:

$$[\eta] = \frac{14}{15} + \frac{q^2}{15(\log 2 \cdot q - 3/2)} + \frac{q^2}{5(\log 2 \cdot q - 1/2)} \qquad \text{(S5)}$$

where [η] is the intrinsic viscosity and q is the axial ratio of the ellipsoid. Using [η] = 47.3 mL/g for CNCs (as calculated from the plot in **Figure S3** according to Equation S5), q ~ 26 for CNCs dispersed in DI water.

Complete Frequency Sweep and Complex Viscosity Data for 6 wt% PVA-SbQ Solutions Containing Dispersed CNCs

The frequency sweep and complex viscosity data for all concentrations of CNCs (0-2.5 wt%) dispersed in 6 wt% PVA-SbQ are provided for completeness in **Figure S4**.

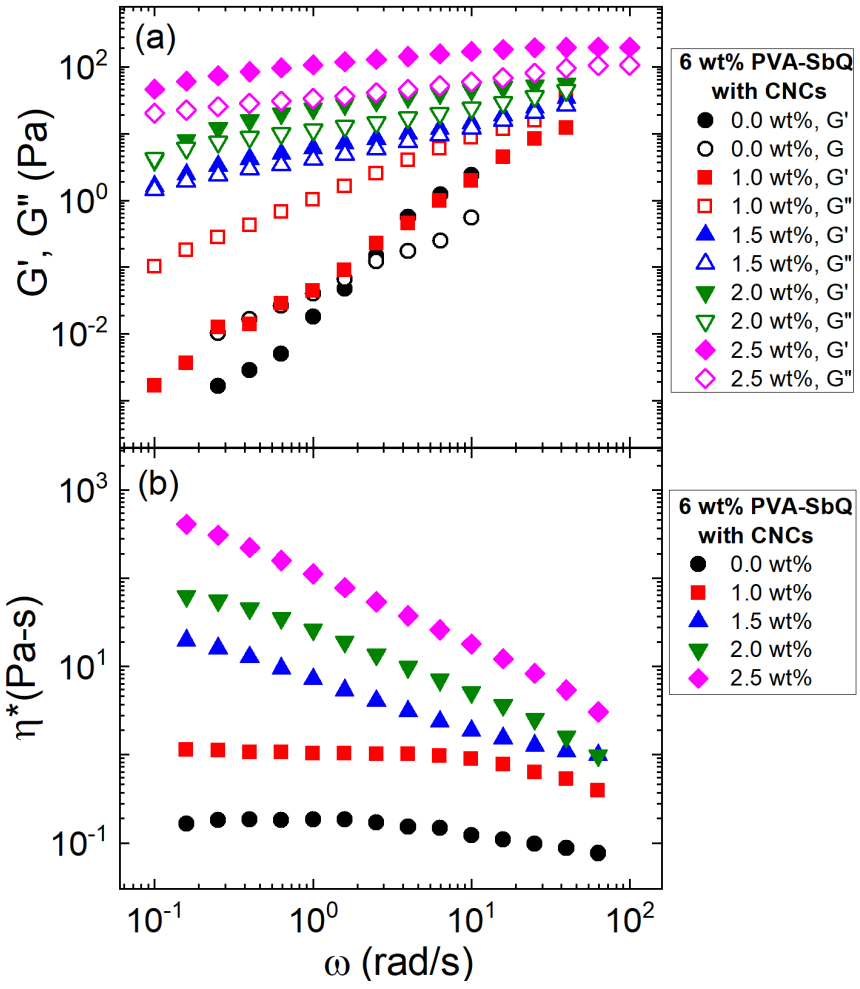

Figure S4. (a) Storage and loss moduli (filled symbols = G' and open symbols = G") and (b) complex viscosity (η*) versus frequency (ω), for 6 wt% PVA-SbQ containing CNCs up to 2.5 wt% (data sets labeled and color-coded).

Power-law Model Fitting of Complex Viscosity Data for 6 wt% PVA-SbQ Solutions Containing Dispersed CNCs

The complex viscosity (η*) data displayed in **Figure 3b**, can be fitted to a power-law model according to Equation S6 at frequencies (ω) above an onset frequency required for shear-thinning:

$$\eta^* = A\omega^{n-1} \quad \text{(S6)}$$

where A is a scalar prefactor and n is the flow behavior index. Smaller values of n indicate a greater degree of shear-thinning behavior. The fitting parameters are given below in **Table S1**. The onset frequency for shear-thinning was selected as the minimum frequency required to maximize the coefficient of determination (R^2).

Table S1. Power-law parameters (onset frequency (ω), scalar prefactor (A), and flow behavior index (n)) for 6 wt% PVA-SbQ with CNCs at different concentrations (data from **Figure 3b**).

CNC (wt%)	Onset ω (rad/s)	A (Pa s^n rad^{1-n})	n	R^2
0	10.0	0.219	0.747	0.999
1.0	10.0	2.35	0.587	0.986
1.5	0.25	7.25	0.418	0.998
2.0	0.25	24.9	0.385	0.995
2.5	0.16	117	0.348	0.995

Steady-Shear Rheology for 6 wt% PVA-SbQ Solutions Containing Dispersed CNCs and Herschel-Bulkley Model Fitting

Steady-shear rheology data (shear rate range 10^0 – $2x10^3$ s^{-1}) for 6 wt% PVA-SbQ at varying CNC loading levels is presented in **Figure S5**. Low concentrations of CNCs (< 1.5 wt%) display Newtonian flow behavior, with visible non-linear deviations arising at concentrations above 1.5 wt.%. This non-linear behavior can be fitted to a Herschel-Bulkley model, given below as Equation S7:

$$\tau = \tau_0 + k\dot{\gamma}^n \qquad \text{(S7)}$$

where τ_0 is the yield stress, k is the consistency index, and n is the flow behavior index. The fitting results, tabulated in **Table S2**, reveal an absence of an apparent yield stress for CNC concentrations below 1.5 wt%, with τ_0 values varying between 0.01 Pa to 0.06 Pa. Above 1.5 wt% CNCs, however, a measurable increase in τ_0 is observed to 1.14 Pa for 1.8 wt% CNCs, which further increases to 8.61 Pa for 2.1 wt% CNCs. Additionally, systems above the threshold concentration of 1.5 wt% CNCs exhibited a high degree of shear thinning (n = 0.572 and 0.455 for 1.8 and 2.1 wt% CNCs, respectively), along with higher values of k.

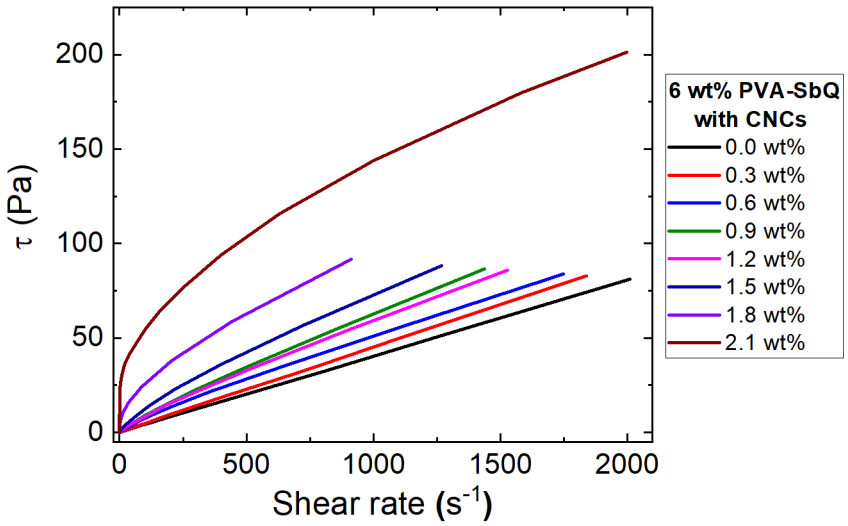

Figure S5. Plot of shear stress (τ) as a function of shear rate for 6 wt% PVA-SbQ with different CNC concentrations between 0 and 2.1 wt% (lines labeled and color-coded).

Table S2. Herschel-Bulkley parameters (yield stress (τ_0), consistency index (k), and flow-behavior index (n)) for 6 wt% PVA-SbQ containing varying amounts of CNCs.

CNC (wt%)	τ_0 (Pa)	k (Pa s^n)	n	R^2
0	0.06	0.04	0.998	0.999
0.3	0.06	0.05	0.987	0.999
0.6	0.01	0.14	0.859	0.999
0.9	0.02	0.16	0.862	0.999
1.2	0.02	0.17	0.852	0.999
1.5	0.05	0.36	0.771	0.999
1.8	1.14	1.81	0.572	0.997
2.1	8.61	5.88	0.455	0.992

Approximation of the Gel Point Concentration of CNCs in 6 wt% PVA-SbQ using the Winter-Chambon Criterion

According to the Winter-Chambon criterion, the loss tangent (tan δ = G"/G') exhibits frequency (ω) independence at the gel point.[9,10] tan δ values were extracted from the frequency sweep data in **Figure 3a** and are plotted below as a function of CNC concentration at four different frequencies. The data sets intersect at ~1.5 wt% CNCs, which can be taken as an approximation of the gel point. The critical relaxation exponent (Δ) can be determined from the value of tan δ at the gel point using Equation S8:

$$\tan\delta = \tan\left(\frac{\Delta\pi}{2}\right) \qquad \text{(S8)}$$

Using tan δ = 0.786 ± 0.086 for 1.5 wt% CNCs, we obtain Δ = 0.423 ± 0.034 at the gel point. This value of Δ is close to that observed by Du and Hill (Δ ≈ 0.38) for weakly-crosslinked polyacrylamide hydrogels close to the percolation threshold.[11]

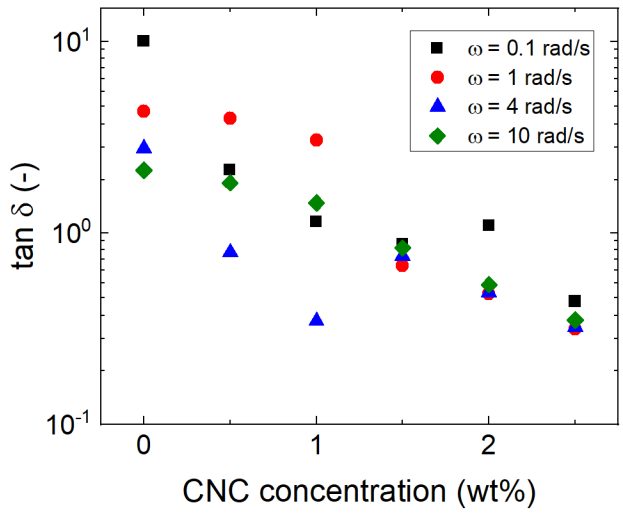

Figure S6. Approximation of the gel point concentration for 6 wt% PVA-SbQ with added CNCs using the Winter-Chambon criterion (data sets labeled and color-coded).

G' Scaling with CNC Loading Prior to Photocrosslinking

Values of G' (at a frequency of 1 rad/s) for 6 wt% PVA-SbQ solutions with CNC loadings ≥ 1.5 wt% were extracted from **Figure S4a** and are plotted with respect to CNC mass fraction in **Figure S7**. From this plot, a scaling exponent of 4.55 can be extracted, which falls squarely within the theoretical limits of 11/3 and 7 established by Hill for entangled microfibrillar cellulose gels.[12] This indicates that interactions between percolated CNCs and PVA-SbQ increase network stiffness prior to photocrosslinking by functioning as additional entanglement points between PVA-SbQ chains.

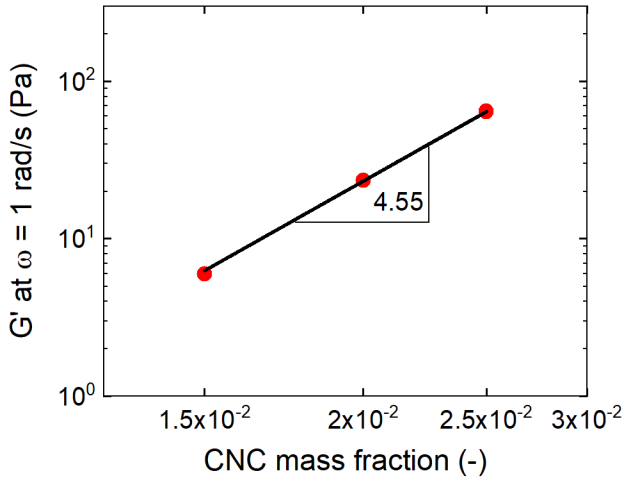

Figure S7. Values of G' (at frequency ω = 1 rad/s) versus CNC mass fraction for 6 wt% PVA-SbQ at CNC loadings at and above the percolation threshold of 1.5 wt%. The solid black line depicts a power-law fit to the data.

References

1 H. Chang, J. Luo, A. A. Bakhtiary Davijani, A. T. Chien, P. H. Wang, H. C. Liu and S. Kumar, *ACS Appl. Mater. Interfaces*, 2016, **8**, 5768–5771.

2 J. G. Kirkwood and J. Riseman, *J. Chem. Phys.*, 1948, **16**, 565–573.

3 V. A. Davis, L. M. Ericson, A. N. G. Parra-Vasquez, H. Fan, Y. Wang, V. Prieto, J. A. Longoria, S. Ramesh, R. K. Saini, C. Kittrell, W. E. Billups, W. W. Adams, R. H. Hauge, R. E. Smalley and M. Pasquali, *Macromolecules*, 2004, **37**, 154–160.

4 E. E. Ureña-Benavides, G. Ao, V. A. Davis and C. L. Kitchens, *Macromolecules*, 2011, **44**, 8990–8998.

5 S. Shafiei-Sabet, W. Y. Hamad and S. G. Hatzikiriakos, *Langmuir*, 2012, **28**, 17124–17133.

6 M.-C. Li, Q. Wu, K. Song, S. Lee, Y. Qing and Y. Wu, *ACS Sustain. Chem. Eng.*, 2015, **3**, 821–832.

7 M. L. Huggins, *J. Am. Chem. Soc.*, 1942, **64**, 2716–2718.

8 R. Simha, *J. Phys. Chem.*, 1940, **44**, 25–34.

9 H. H. Winter and F. Chambon, *J. Rheol.*, 1986, **30**, 367–382.

10 F. Chambon and H. H. Winter, *J. Rheol.*, 1987, **31**, 683–697.

11 C. Du and R. J. Hill, *J. Rheol.*, 2019, **63**, 109–124.